Orbital susceptibility of higher-stage graphite intercalation compounds

doi: 10.1103/PhysRevB.33.7218

Orbital susceptibility of higher-stage graphite intercalation compounds

R. Saito and H. Kamimura
Department of Physics, University of Tokyo, Bunkyo-ku, Tokyo 113, Japan
(Received 23 September 1985)

The calculated results of the orbital susceptibility for first- to fifth-stage graphite intercalation compounds (GIC's) are presented. In this calculation a new formalism for calculating the orbital susceptibility is presented. Furthermore, in order to perform calculations in an analytical way, the effective Hamiltonian for reproducing the band structures of higher-stage GIC's is introduced. In this Hamiltonian the effects of the inhomogeneous charge distribution along the c axis in higher-stage GIC's and the interlayer interactions are taken into account within a thin-film model. It is shown that the interband effects between π bands split by the inhomogeneous charge distribution plays an essential role in determining the stage dependence of orbital susceptibility. Calculated results of the stage dependence of orbital susceptibility with charge transfer $f=1.0$ and $f=0.3$ are in good agreement with observed ones.

I. INTRODUCTION

The magnetic susceptibility of graphite intercalation compounds (GIC's) is a powerful tool for investigating the c-axis charge distribution of carriers in the graphite layers transferred from intercalant layers, especially in exploring its stage dependence, because the stage dependence is sensitive to the c-axis charge distribution. The anisotropic behavior of the magnetic susceptibility of alkali GIC's was first measured by DiSalvo *et al.*[1] Their result was very striking in the sense that the orbital susceptibility in a magnetic field parallel to the c axis is paramagnetic and increases its paramagnetic value with increasing stage number from 1 to 4. It is well known that the orbital susceptibility of normal metals is diamagnetic and that pristine graphite exhibits an anomalously large diamagnetism because of interband effects between bonding and antibonding π bands.[2,3] In this view the paramagnetic orbital susceptibility of GIC's is very exotic in connection with the electronic and structural[1,4] change from pristine graphite to GIC's. Recently Suda and Suematsu measured the susceptibility up to the eighth stage and found that the orbital susceptibility has a maximum value at the fourth stage and then decreases and becomes diamagnetic at the seventh stage.[5] In order to clarify the origin of such unusual behavior of the orbital susceptibility in GIC's, Safran and DiSalvo calculated the orbital susceptibility of GIC's with the model of a single graphite layer,[6,7] starting from the rigorous formula for the orbital susceptibility derived by Fukuyama.[8] In their calculation, the band structure of a single graphite layer is given by a simple two-dimensional tight-binding model. Their results for the susceptibility as a function of the Fermi energy seemed to succeed in explaining the observed stage dependence of the orbital susceptibility. Later, however, Blinowski and Rigaux[9] obtained a different result at small values of the Fermi energy, starting from the same model that Safran and DiSalvo adopted, and claimed that numerical calculations by Safran and DiSalvo were inaccurate at small values of the Fermi energy, although the mechanism proposed by Safran and DiSalvo for the unusual paramagnetic susceptibility was correct for larger values of the Fermi energy. According to the result of Blinowski and Rigaux, the orbital susceptibility does not depend on stage number, therefore the observed stage dependence of the orbital susceptibility cannot be explained by the simple tight-binding model of a single graphite layer.

In this same light we have noticed that the effect of the inhomogeneous charge distribution along the c axis, which neither Safran and DiSalvo nor Blinowski and Rigaux took into account, is essential in giving rise to the stage dependence of the orbital susceptibility. Thus, in this paper we take into account the effect of the inhomogeneous charge distribution, and calculate the orbital susceptibility for first- and fifth-stage GIC's for charge transfer $f=1.0$.

Very recently Safran calculated the susceptibility of second stage GIC's,[10] using a linear energy dispersion for π bands along the graphite layer and taking into account the interlayer interaction between graphite layers, γ_1. The result shows that the interlayer interaction between two graphite layers contributes to the orbital paramagnetism in the second-stage case. In the higher-stage GIC's, the bonding and antibonding π bands are further split by electrostatic interactions due to the transferred charge from intercalant layers and coupled to each other in a complex manner near the Fermi energy. Thus, various kinds of interlayer interaction in the complex energy dispersions of π bands in the higher stage GIC's should be considered so as to calculate the orbital susceptibility. In this view the susceptibility calculations of higher stage GIC's are so complicated that supercomputers are necessary.

In the next section we first formulate a theoretical approach for calculating the orbital susceptibility in the system of multienergy bands. Then in order to apply this approach to higher stage GIC's, we introduce an effective Hamiltonian which reproduces the π-band structure of higher stage GIC's. Using the effective Hamiltonian, the orbital susceptibility is calculated in an analytical way. In

Sec. III we present the numerical results of the orbital susceptibility for the first- to fifth-stage GIC's in the case of charge transfer $f=1.0$. Through the analysis of numerical results we try to clarify the effects of intraband and interband interactions on the orbital susceptibility. In Sec. IV we present the numerical results of orbital susceptibility of the third- and fourth-stage GIC's for $f=0.3$. Comparing the results of $f=0.3$ with those of $f=1.0$, the effects of charge distribution on orbital susceptibility are investigated. Both theoretical results of $f=1.0$ and $f=0.3$ are compared with experimental results in Secs. III and IV. In Sec. V, the main results obtained in this paper are summarized.

II. FORMULATION

In this section we develop a theoretical formulation which is suitable to the present system. This new formulation is general in the sense that it is applicable to not only GIC's but also other metals which have multidegenerate band structures at the Fermi level.

We start from the rigorous formula for orbital susceptibility χ_{or} derived by Fukuyama,[8]

$$\chi_{or}=(e/\hbar c)2k_BT\frac{1}{8\pi^3}\sum_n\int dk\,[\mathrm{Tr}(\gamma_x g\gamma_y g\gamma_x g\gamma_y g)]\ , \tag{1}$$

where g is Matsubara's Green function defined by

$$g=(\epsilon_n I-\mathscr{H})^{-1}\ , \tag{2}$$

with

$$\epsilon_n=(2n+1)\pi i k_BT+\mu \qquad (n=\ldots,-2,\ -1,\ 0,\ 2,\ \ldots)\ , \tag{3}$$

(Ref. 11) and μ is the chemical potential. The matrices I and $\mathscr{H}$ are a unit matrix and Hamiltonian matrix, respectively. The matrices γ_x and γ_y are the momentum operators multiplied by $\hbar/m$ which are given by

$$\gamma_x=\frac{\partial}{\partial k_x}\mathscr{H}\ \text{ and }\ \gamma_y=\frac{\partial}{\partial k_y}\mathscr{H}\ , \tag{4}$$

respectively. This representation of momentum matrices is valid within the tight-binding approximation.

For nth-stage GIC's to which Eq. (1) is going to be applied, we consider a system which consists of n graphite layers bounded by the intercalant charged sheets. In the Hamiltonian for this system, not only the intralayer interactions but also interlayer interactions are taken into account. As a result, $2n$-dimensional matrices must be considered for $\mathscr{H}$, γ_x, γ_y, and g, where $2n$ is number of π bands. In applying Eq. (1) to this system we transform Eq. (1) by a unitary matrix U so as to diagonalize the Hamiltonian matrix and thus the Green function for the present system. For this purpose we can choose the unitary matrix U in such a way that it is not a function of ϵ_n but only of k_x and k_y. The resulting expression for χ_{or} is

$$\chi_{or}=(e/\hbar c)2k_BT\frac{1}{8\pi^3}\sum_n\int dk\,[\mathrm{Tr}(U^{-1}\gamma_x U\tilde{g}U^{-1}\gamma_y U\tilde{g}U^{-1}\gamma_x U\tilde{g}U^{-1}\gamma_y U\tilde{g})]\ , \tag{5}$$

where

$$\begin{aligned}\tilde{g}&=U^{-1}gU\\&=U^{-1}(\epsilon_n I-\mathscr{H})^{-1}U\\&=(\epsilon_n I-U^{-1}\mathscr{H}U)^{-1}\\&=\begin{bmatrix}1/[\epsilon_n-E_1(k_x,k_y)] & & \\ & \ddots & \\ & & 1/[\epsilon_n-E_N(k_x,k_y)]\end{bmatrix}.\end{aligned} \tag{6}$$

Here, $E_i(k_x,k_y)$ is the ith eigenvalue of the Hamiltonian matrix, N is the total number of π bands, that is twice the stage number, and the trace in the integrand is taken over the band indices i, j, k, and l. As a result of unitary transformation we can express the integrand $[\cdots]$ in Eq. (5) in the following form:

$$[\cdots]=\sum_{i,j,k,l=1}^{N}F(i,j,k,l)G(i,j,k,l)\ , \tag{7}$$

where

$$F(i,j,k,l)=1/[(\epsilon_n-E_i)(\epsilon_n-E_j)(\epsilon_n-E_k)(\epsilon_n-E_l)]\ , \tag{8}$$

$$G(i,j,k,l)=X_{ij}Y_{jk}X_{kl}Y_{li}\ , \tag{9}$$

with

$$X_{ij}=(U^{-1}\gamma_x U)_{ij}\ \text{ and }\ Y_{ij}=(U^{-1}\gamma_y U)_{ij}\ . \tag{10}$$

It is noted that F, G, X, and Y are functions of k_x and k_y.

Furthermore, the term $F(i,j,k,l)$ can be decomposed into partial fractions. The way of decomposing F into partial fractions is different for the following five cases.

For case (i), $i=j=k=l$,

$$F(i,i,i,i)=\frac{1}{(\epsilon_n-E_i)^4}\ , \tag{11}$$

for case (ii), $i=j=k\neq l$,

$$F(i,i,i,j)=\frac{1}{(\epsilon_n-E_i)^3(\epsilon_n-E_j)}$$
$$=\frac{1}{(E_i-E_j)^3(\epsilon_n-E_i)}-\frac{1}{(E_i-E_j)^2(\epsilon_n-E_i)^2}$$
$$+\frac{1}{(E_i-E_j)(\epsilon_n-E_i)^3}-\frac{1}{(E_i-E_j)^3(\epsilon_n-E_j)}\ , \tag{12}$$

for case (iii), $i=j\neq k=l$,

$$F(i,i,j,j)=\frac{1}{(\epsilon_n-E_i)^2(\epsilon_n-E_j)^2}$$
$$=\frac{-2}{(E_i-E_j)^3(\epsilon_n-E_i)}+\frac{1}{(E_i-E_j)^2(\epsilon_n-E_i)^2}$$
$$+\frac{2}{(E_i-E_j)^3(\epsilon_n-E_j)}+\frac{1}{(E_i-E_j)^2(\epsilon_n-E_j)^2}\ . \tag{13}$$

for case (iv), $i=j\neq k\neq l$,

$$F(i,i,j,k)=\frac{1}{(\epsilon_n-E_i)^2(\epsilon_n-E_j)(\epsilon_n-E_k)}$$
$$=\frac{(E_j+E_k-2E_i)}{(E_i-E_k)^2(E_i-E_j)^2(\epsilon_n-E_i)}+\frac{1}{(E_i-E_k)(E_i-E_j)(\epsilon_n-E_i)^2}$$
$$+\frac{1}{(E_j-E_k)(E_i-E_j)^2(\epsilon_n-E_j)}+\frac{1}{(E_k-E_j)(E_i-E_k)^2(\epsilon_n-E_k)}\ , \tag{14}$$

for case (v), $i\neq j\neq k\neq l$,

$$F(i,j,k,l)=\frac{1}{(\epsilon_n-E_i)(\epsilon_n-E_j)(\epsilon_n-E_k)(\epsilon_n-E_l)}$$
$$=\frac{1}{(E_i-E_j)(E_i-E_k)(E_i-E_l)(\epsilon_n-E_i)}+\frac{1}{(E_j-E_i)(E_j-E_k)(E_j-E_l)(\epsilon_n-E_j)}$$
$$+\frac{1}{(E_k-E_i)(E_k-E_j)(E_k-E_l)(\epsilon_n-E_k)}+\frac{1}{(E_l-E_i)(E_l-E_j)(E_l-E_k)(\epsilon_n-E_l)}\ . \tag{15}$$

Since the suffixes i, j, k, and l take a value from 1 to N, there are N^4 terms in $F(i,j,k,l)$. But some of the terms in F are found to give the same contribution to χ_{or} as other terms through the permutation of the suffixes. For example, we have

$$F(1,1,1,2)=F(1,1,2,1)=F(1,2,1,1)=F(2,1,1,1)\ , \tag{16}$$

and

$$F(1,1,2,2)=F(1,2,1,2)=F(1,2,2,1)=F(2,1,1,2)$$
$$=F(2,1,2,1)=F(2,2,1,1)\ldots\ . \tag{17}$$

Since each of the above terms is decomposed into partial fractions, different $G(i,j,k,l)$'s with the same F are brought together into one term. As a result the number of independent terms in F is reduced to $N(N+1)(N+2)(N+3)/4!$. As seen in Eqs. (16) and (17), the number of permutation of suffixes is different for each of the above five cases of F and it is summarized in Table I.

Expressing $F(i,j,k,l)$ in terms of the partial fractions, the integrand $[\cdots]$ in Eq. (5) can be written in the following simple form:

$$[\cdots]=\sum_{m=1}^{N}\sum_{p=1}^{4}\frac{1}{(\epsilon_n-E_m)^p}H(m,p)\ , \tag{18}$$

where $H(m,p)$ is a function consisting of the linear combination of $G(i,j,k,l)$. A definite form of $H(m,p)$ which is calculated by a computer is not shown here because it is too complicated. It is a monotonic function of G. The quantities $G(i,j,k,l)$ represent the contribution from the interband interactions among ith, jth, kth, and lth bands. It is noted that an intraband interaction within the ith band corresponds to $G(i,j,k,l)$ as a special case of $i=j=k=l$. By this formalism the N^4 terms in Eq. (7) are reduced to $4N$ terms in Eq. (18). This reduction becomes very efficient when the stage number $(N/2)$ increases. In fact we could calculate the susceptibility for third, fourth, and fifth stage only by using this reduction formula.

In the expression Eq. (12), the poles of Matsubara's Green function, ϵ_n, appear only in the factor $(\epsilon_n-E_m)^{-p}$ and thus we can easily take the summation over the poles before the integration is carried out. That is,

$$\sum_n\frac{1}{(\epsilon_n-E_m)^p}=\frac{1}{k_BT(p-1)!}\frac{\partial^{p-1}f(E_m)}{\partial E_m^{p-1}}\ , \tag{19}$$

where $f(E_p)$ is the Fermi distribution function. Finally Eq. (1) is reduced to the following simple form:

TABLE I. (A) The number of permutation of suffixes i, j, k, l in a $F(i,j,k,l)$, (B) the number of the independent terms of $F(i,j,k,l)$'s, and (C) the number of $F(i,j,k,l)$'s, that is, (A)×(B), for the five cases of $F(i,j,k,l)$. (N represents the number of energy bands.)

Cases	(A) Number of permutation	(B) Number of kind of F's	(C) Number of F's (A)×(B)
(i) $i=j=k=l$ $[F(i,i,i,i)]$	1	N	N
(ii) $i=j=k\neq l$ $[F(i,i,i,j)]$	4	$N(N-1)$	$4N(N-1)$
(iii) $i=j\neq k=l$ $[F(i,i,j,j)]$	6	$N(N-1)/2$	$3N(N-1)$
(iv) $i=j\neq k\neq l$ $[F(i,i,j,k)]$	12	$N(N-1)(N-2)/2$	$6N(N-1)(N-2)$
(v) $i\neq j\neq k\neq l$ $[F(i,j,k,l)]$	24	$N(N-1)(N-2)(N-3)/4!$	$N(N-1)(N-2)(N-3)$
Total		$N(N+1)(N+2)(N+3)/4!$	N^4

$$\chi_{\rm or}=(e/\hbar c)^2\frac{1}{8\pi^3}\sum_{p=1}^{4}\frac{1}{(p-1)!}\times\sum_{m=1}^{N}\int dk\,H(m,p)\frac{\partial^{p-1}f(E_m)}{\partial E_m^{p-1}}\,. \tag{20}$$

This is a general formula of orbital susceptibility. This is very useful for calculating the orbital susceptibility in the case of multidegenerate energy bands at the Fermi level.

It should be noted here that some partial fractions in Eqs. (11)–(15) include factors such as $(E_i-E_j)^{-p}$ which diverge in the degenerate case such as $E_i=E_j$. But this difficulty is not so serious, because this divergence is caused by decomposing nondivergent terms into partial fractions. Thus, this divergence can be avoided with a special treatment at a degenerate point in the k space.[12]

Next we introduce an effective Hamiltonian which reproduces the band-structure results of higher stage GIC's calculated by the local-density formalism (LDF) method. From the effective Hamiltonian and Eq. (4), the matrix elements of momentum components γ_x and γ_y can be given in the analytical forms. The basis functions for the effective Hamiltonian are taken as the tight-binding wave functions composed of $2p_z$ orbitals of each carbon atom. The effective Hamiltonians for first- to fifth-stage GIC's with these bases are given in the following forms:

For the first stage,

$$\mathscr{H}=\begin{bmatrix}0 & H(k)\\ H^*(k) & 0\end{bmatrix}, \tag{21a}$$

for the second stage,

$$\mathscr{H}=\begin{bmatrix}\delta_1 & H(k) & \gamma_1 & \gamma_4h^*(k)\\ H^*(k) & -\delta_1 & \gamma_4h^*(k) & \gamma_3h(k)\\ \gamma_1 & \gamma_4h(k) & \delta_1 & H^*(k)\\ \gamma_4h(k) & \gamma_3h^*(k) & H(k) & -\delta_1\end{bmatrix}, \tag{21b}$$

for the third stage,

$$\mathscr{H}=\begin{bmatrix}-\delta+\delta_1 & H(k) & \gamma_1 & \gamma_4h^*(k) & 0 & 0\\ H^*(k) & -\delta-\delta_1 & \gamma_4h^*(k) & \gamma_3h(k) & 0 & 0\\ \gamma_1 & \gamma_4h(k) & \delta+\delta_2 & H^*(k) & \gamma_1 & \gamma_4h(k)\\ \gamma_4h(k) & \gamma_3h^*(k) & H(k) & \delta-\delta_2 & \gamma_4h(k) & \gamma_3h^*(k)\\ 0 & 0 & \gamma_1 & \gamma_4h^*(k) & -\delta+\delta_1 & H(k)\\ 0 & 0 & \gamma_4h^*(k) & \gamma_3h(k) & H^*(k) & -\delta-\delta_1\end{bmatrix}, \tag{21c}$$

for the fourth stage,

$$\mathcal{H}=\begin{pmatrix}
-\delta+\delta_1 & H(k) & \gamma_1 & \gamma_4 h^*(k) & 0 & 0 & 0 & 0 \\
H^*(k) & -\delta-\delta_1 & \gamma_4 h^*(k) & \gamma_3 h(k) & 0 & 0 & 0 & 0 \\
\gamma_1 & \gamma_4 h(k) & \delta+\delta_2 & H^*(k) & \gamma_1 & \gamma_4 h(k) & 0 & 0 \\
\gamma_4 h(k) & \gamma_3 h^*(k) & H(k) & \delta-\delta_2 & \gamma_4 h(k) & \gamma_3 h^*(k) & 0 & 0 \\
0 & 0 & \gamma_1 & \gamma_4 h^*(k) & \delta+\delta_2 & H(k) & \gamma_1 & \gamma_4 h^*(k) \\
0 & 0 & \gamma_4 h^*(k) & \gamma_3 h(k) & H^*(k) & \delta-\delta_2 & \gamma_4 h^*(k) & \gamma_3 h(k) \\
0 & 0 & 0 & 0 & \gamma_1 & \gamma_4 h(k) & -\delta+\delta_1 & H^*(k) \\
0 & 0 & 0 & 0 & \gamma_4 h(k) & \gamma_4 h^*(k) & H(k) & -\delta-\delta_1
\end{pmatrix}, \tag{21d}$$

for the fifth stage,

$$\mathcal{H}=\begin{pmatrix}
-\delta+\delta_1 & H(k) & \gamma_1 & \gamma_4 h^*(k) & 0 & 0 & 0 & 0 & 0 & 0 \\
H^*(k) & -\delta-\delta_1 & \gamma_4 h^*(k) & \gamma_3 h(k) & 0 & 0 & 0 & 0 & 0 & 0 \\
\gamma_1 & \gamma_4 h(k) & \delta'+\delta_2 & H^*(k) & \gamma_1 & \gamma_4 h(k) & 0 & 0 & 0 & 0 \\
\gamma_4 h(k) & \gamma_3 h^*(k) & H(k) & \delta'-\delta_2 & \gamma_4 h(k) & \gamma_3 h^*(k) & 0 & 0 & 0 & 0 \\
0 & 0 & \gamma_1 & \gamma_4 h^*(k) & \delta''+\delta_3 & H(k) & \gamma_1 & \gamma_4 h^*(k) & 0 & 0 \\
0 & 0 & \gamma_4 h^*(k) & \gamma_3 h(k) & H^*(k) & \delta''-\delta_3 & \gamma_4 h^*(k) & \gamma_3 h(k) & 0 & 0 \\
0 & 0 & 0 & 0 & \gamma_1 & \gamma_4 h(k) & \delta'+\delta_2 & H^*(k) & \gamma_1 & \gamma_4 h(k) \\
0 & 0 & 0 & 0 & \gamma_4 h(k) & \gamma_3 h^*(k) & H(k) & \delta'-\delta_2 & \gamma_4 h(k) & \gamma_3 h^*(k) \\
0 & 0 & 0 & 0 & 0 & 0 & \gamma_1 & \gamma_4 h^*(k) & -\delta+\delta_1 & H(k) \\
0 & 0 & 0 & 0 & 0 & 0 & \gamma_4 h^*(k) & \gamma_3 h(k) & H^*(k) & -\delta-\delta_1
\end{pmatrix}, \tag{21e}$$

with

$$h(k)=H(k)/\gamma_0 . \tag{22}$$

Here $H(k)$ represents the nearest-neighbor transfer interaction. Matrix elements δ, δ_1, and δ_2 represent the difference between site energies of certain sites due to the inhomogeneous charge distribution, while γ_0, γ_1, γ_3, and γ_4 represent the transfer integrals between some neighboring sites. The relations between these matrix elements and corresponding sites are shown in Fig. 1. Hereafter we call these matrix elements the band parameters. Without the band parameters γ_3 and γ_4, the effective Hamiltonian is the same as that proposed by Blinowski *et al.*[13,14]

Here we would like to point out an important role of band parameters γ_3 and γ_4 in determining the orbital susceptibility. These band parameters correspond to the transfer integrals between the carbon atoms in the adjacent layers, and thus represent the interlayer interactions. Although their values are small, these interactions give significant contribution to χ_{or}, because these interactions cause the mixing of the orbital angular momentum by the orbital motion of an electron through various sites of different layers around a magnetic field. In fact, these band parameters in the effective Hamiltonian give rise to the nonvanishing momentum matrix elements of γ_x and γ_y, and contribute to χ_{or}.

All of the band parameters are determined so as to reproduce the energy bands calculated numerically by Ohno and Kamimura[15] with the LDF. In reproducing the energy bands we have made the least-square fit. Since it is not easy to find the optimum value of the least-square fit for all of the band parameters simultaneously, we first determine some of them at the K point where $H(k)$ vanishes. The other band parameters are then determined at other symmetry points in the Brillouin zone such as M points. The band parameters we used are listed in Table II. It should be pointed out that overlap integrals between neighboring carbon atoms are neglected for simplicity. In fact, near the Fermi energy the effect of overlap integrals is small, and it can be considered that the band parameters implicitly include the effect of the overlap integral by fitting the effective Hamiltonian to the first-principles calculation.

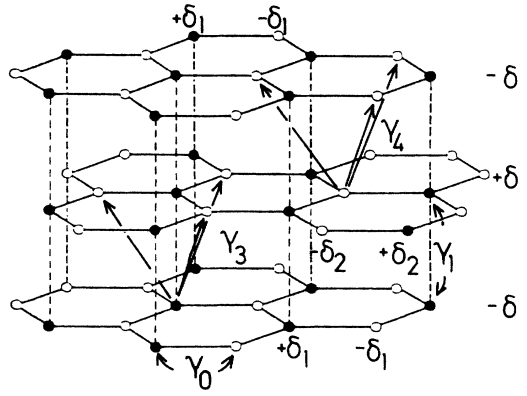

FIG. 1. Band parameters of the effective Hamiltonian: δ, δ_1, and δ_2, are the parameters which represent different site energies, and γ_0, γ_1, γ_3, and γ_4 represent the transfer integrals between various neighboring atoms.

TABLE II. Band parameters of the effective Hamiltonian for the case of the charge transfer $f=1.0$ and $f=0.3$ which are fitted to π-band structures of the higher stage GIC's by Ohno and Kamimura (Ref. 15). Units are in eV.

			$f=1.0$			$f=0.3$	
Parameters	Stage 1	Stage 2	Stage 3	Stage 4	Stage 5	Stage 3	Stage 4
γ_0	3.11	3.30	3.30	3.30	3.30	3.30	3.30
γ_1		0.320	0.320	0.320	0.320	0.254	0.254
γ_3, γ_4		0.210	0.210	0.210	0.210	0.200	0.200
δ			0.467	0.469	0.442	−0.195	−0.145
δ'					−0.576		
δ''					−0.916		
δ_1			−0.018	−0.010	−0.019	−0.035	−0.010
δ_2			−0.011	−0.001	−0.048	−0.025	−0.008
δ_3					−0.033		

The numerical integration in the formula Eq. (20) for χ_{or} was performed in a rectangle section in the extended zone of the reciprocal lattice, as shown in Fig. 2. This section is equivalent to the hexagon of the first Brillouin zone. Furthermore we can easily show that the integration for the upper half and the lower half of the section gives the same contribution to the susceptibility because of twofold symmetry of $H(k)$ and its derivatives with regard to k_y. Since the integrand in Eq. (20) includes the derivative of the Fermi distribution function, we have taken the following fine care of accuracy in computation. In order to perform computations, we have divided first the upper half of the rectangle section into 330×200 meshes. each mesh is further divided into 16×16 meshes when the mesh is located in the energy region of $80k_BT$ around the Fermi energy in the two-dimensional (2D) Brillouin zone. Thus we have taken the sampling points of about 5×10^6 to 8×10^6. As a whole we have taken a great deal of sampling points in the process of integration such as $330\times200\times16\times16=3.3\times10^7$ points. At each point we have calculated all of the interband contributions to the orbital susceptibility where the temperature is taken to be 300 K. This kind of computation becomes possible with the use of a computer with parallel processors; a so-called supercomputer. Thus, the present computation was realized by using a supercomputer, HITAC S810, of the University of Tokyo.

III. CALCULATED RESULTS FOR $f=1.0$ AND COMPARISON WITH EXPERIMENTS

In Fig. 3 we present the calculated results of the orbital susceptibility χ_{or} as a function of the Fermi energy together with the energy dispersion of π bands near the K point for the first- to fifth-stage GIC's with charge transfer $f=1.0$. We explain how to look at the upper half of the figure. The curve of the upper half indicates χ_{or} as a function of E_F. Strictly speaking, when E_F changes, the energy bands should be recalculated self-consistently for the charge transfer corresponding to that Fermi energy. The band structure of a lower part is obtained for E_F corresponding to $f=1.0$. Thus, in the case of $f=1.0$ the results are exact. For other values of E_F we take the rigid-band approximation and sweep simply the Fermi energy without changing the band structure. With this approximation we can discuss the contribution due to the interband interactions. The result of χ_{or} for the first stage just reproduces that of Blinowski and Rigaux. For the second stage, there are two antibonding π^* bands and two bonding π bands. The lower conduction band and upper valence band are degenerate at the K point, as seen in Fig. 3(b). The upper conduction band at the K point is situated above the lower conduction band by the energy γ_1 and the lower valence band lies below the upper valence band by γ_1. The orbital susceptibility for the second stage has a peak if the Fermi energy happens to appear near the bottom of the upper conduction band. The peak represents the effect of the interband interaction between upper and lower conduction bands. A similar result was obtained by Safran[10] with the use of the linear energy

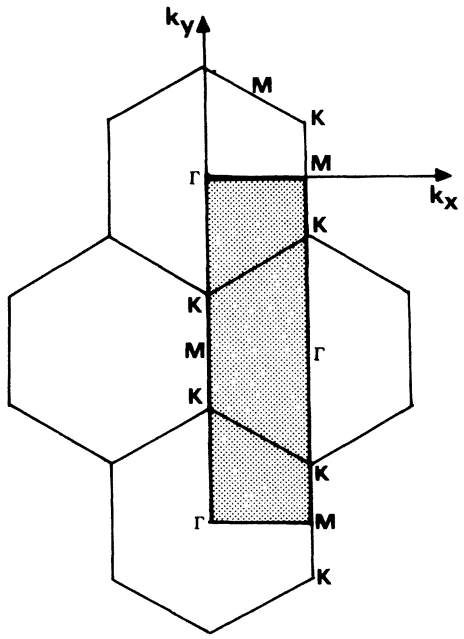

FIG. 2. Rectangle section in the extended zone of the reciprocal lattice adopted for the numerical integration. This section is equivalent to the hexagon of the first Brillouin zone.

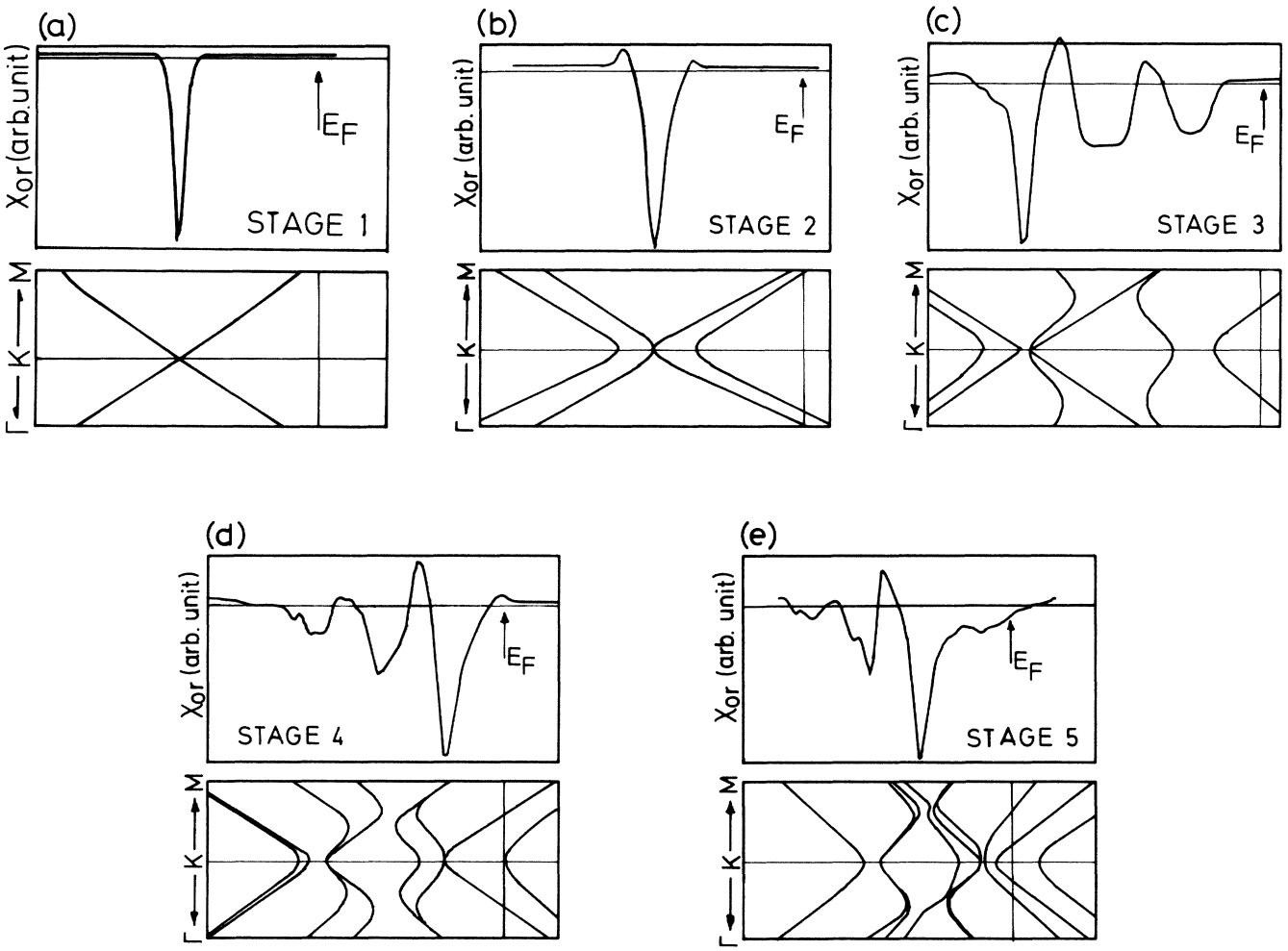

FIG. 3. Numerical results of the orbital susceptibility in arbitrary units as a function of Fermi energy (upper part), and the expanded section of the energy dispersion near the K point for the first to fifth stage GIC's with charge transfer $f=1.0$; (a) first stage, (b) second stage, (c) third stage, (d) fourth stage, and (e) fifth stage (lower part).

dispersion for graphite π bands and by taking into account only the effect of γ_1. Since the band structure has been solved self-consistently for the case of the charge transfer $f=1.0$, a real E_F corresponds to the case of $f=1.0$. Such E_F is marked in Fig. 3(b). It is far above the peak position. Thus in this case the interband effect does not play an important role and that the intraband effect mainly determines χ_{or}. The value of χ_{or} is larger than that of the first stage and this is due to the effects of γ_3 and γ_4 terms which do not exist in the first stage.

We discuss the effect of γ_3 and γ_4 terms. Suppose we neglect the γ_3 and γ_4 matrix elements in the effective Hamiltonians (15) and (16). In that case we have to determine the band parameters, only by fitting the energy bands in the effective Hamiltonian to the energy band positions at the K point in Ohno-Kamirua's band structure. The obtained band structure is shown in Fig. 4. We notice that this band structure does not reproduce the overall feature of energy dispersion in Ohno-Kamimura's band structure. Thus it is pointed out that the γ_3 and γ_4 matrix elements play an essential role in determining the curvature of π bands correctly. Generally the susceptibility is very sensitive to the band curvature and the relative position of the energy bands which govern mainly X_{ij}, Y_{ij}, and E_i-E_j in Eq. (8) and Eqs. (11)–(15). In the case of stage 2, the energy separation between two antibonding π bands due to γ_1 at the K point is reduced by the effect of γ_3 and γ_4 at the Fermi energy corresponding to the case of $f=1.0$. The reduction of the energy separation of π bands at higher energy than that of the K point induces the enhancement of interband interaction of the orbital susceptibility between these two bands. As a result χ_{or} calculated without γ_3 and γ_4 terms is different from that calculated with inclusion of γ_3 and γ_4 terms by about 9%. Physically the inclusion of γ_3 and γ_4 terms induces an orbital motion of an electron over different layers. Consequently an additional orbital angular momentum is created. This contributes to the enhancement of orbital paramagnetism in the higher stage GIC's.

For the third stage, there appear one upper conduction band and two lower conduction bands, as seen in Fig. 3(c). These conduction bands originate from the antibonding

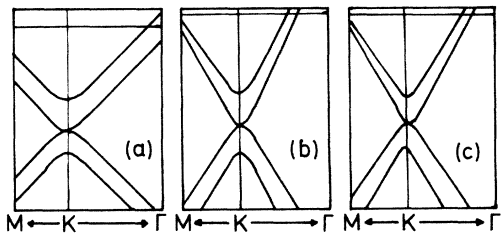

FIG. 4. Comparison of the π-band structures of the second stage near the K point with and without inclusion of γ_3 and γ_4 terms: (a) π-band structure for $\gamma_3=\gamma_4=0$, (b) that with $\gamma_3=\gamma_4\neq 0$, (c) π-band structure calculated by Ohno and Kamimura (Ref. 15).

π^* band in a single graphite layer. The splitting of these bands is due to the inhomogeneous c-axis charge distribution, and it is expressed as the diagonal matrix element δ in the effective Hamiltonian. We have also one upper valence band and two lower valence bands. The highest π^* band corresponds to an interior graphite layer in which the excess charge due to the charge transfer is very small while two lower conduction bands correspond to the bounding graphite layers. Near the K point some of these bands are mixed by the interlayer interactions. Only a pair of one lower conduction band and one higher valence band keeps the linear energy dispersion by the symmetry of the Hamiltonian. The form of orbital susceptibility as a function of the Fermi energy is different from those of the first and second stages. It oscillates as a function of the Fermi energy.

The orbital susceptibility in the third stage at a real Fermi energy corresponding to $f=1.0$ is enhanced from that of the first stage. This is due to interband interactions between lower conduction bands which cross the Fermi level. These lower conduction bands correspond to symmetric and antisymmetric combinations of the states belonging to two bounding graphite layers. In spite of wide separation between two bounding layers in a real space, the energy bands belonging to two bounding graphite layers are nearly degenerate in the k space. Thus large interband interactions between these two bands appear through the interlayer interactions with γ_3 and γ_4 terms. These interactions contribute to orbital paramagnetism. In fact the calculated value of the orbital susceptibility without γ_3 and γ_4 terms in the case of the third stage are almost the same as that in the case of the first stage within 2% in the unit emu/1 C mole. Furthermore it is noted here that the orbital susceptibility of the third stage does not have a peak at the energy position corresponding to the bottom of the highest conduction band, in contrast to the second stage.

For the fourth stage, there are four conduction and four valence bands as seen in Fig. 3(d). The upper two conduction bands are related to the equivalent interior layers and they are separated in energy by γ_1. The orbital susceptibility in this case also oscillates as a function of the Fermi energy and has a peak near the bottom of the upper conduction bands where a real Fermi level corresponding to $f=1.0$ exists. The occurrence of this peak is due to the interlayer interactions. Thus, the orbital susceptibility of the fourth stage is enhanced by the interlayer interactions.

For the fifth stage, a real Fermi energy corresponding to $f=1.0$ is located in the energy gap region below the highest conduction bands, as shown in Fig. 3(e). In this case the highest conduction band which belongs to the innermost layer may be considered as the same as the π^* band of pure graphite and thus the contribution of χ_{or} from the innermost layer is diamagnetic with a large negative value. Hence, the total orbital susceptibility of the fifth stage changes to be diamagnetic.

The calculated stage dependence of the orbital susceptibility for the first to fifth stage is shown in Fig. 5, where experimental results of DiSalvo *et al.* and of Suda and Suematsu and theoretical results by Blinowski and Rigaux on the single graphite layer model are also shown for comparison. The calculated orbital susceptibility in this paper increases its paramagnetic value from first to fourth stage and then decreases to become diamagnetic at the fifth stage. In recent experiments by Suda and Suematsu they also found the occurrence of the maximum at the fourth stage in the stage dependence of χ_{or}, consistent with the prediction of the present theoretical results. Thus, as far as the stage dependence is concerned, the present calculated result is in good agreement with experimental results. Regarding the absolute magnitude, however, there is a large discrepancy between theory and experiment. One of the reasons for this discrepancy is due to the estimation of the magnitude of core susceptibility in the experimental analysis. The experimental values of the orbital susceptibility for potassium GIC's have been obtained by subtracting the Pauli susceptibility χ_{Pauli} and core susceptibility χ_{core} from the measured susceptibility χ_{tot}. That is,

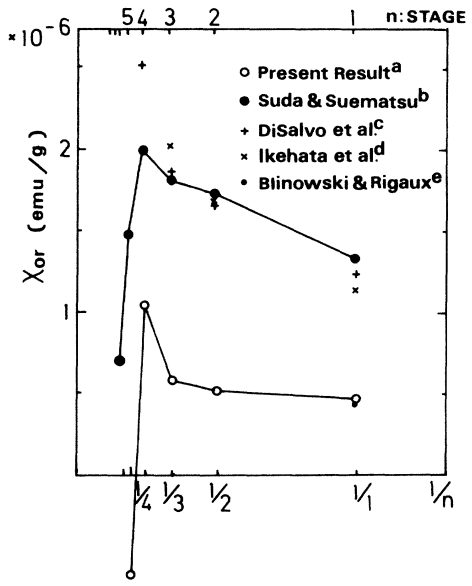

FIG. 5. Calculated stage dependence of the orbital susceptibility (emu/g) versus the inverse of the stage number for the first to fifth stage with charge transfer $f=1.0$. Solid lines are a guide to eye. (a) Present results, (b) see Ref. 5, (c) see Ref. 1, (d) see Ref. 17, (e) see Ref. 9.

$$\chi_{or}=\chi_{tot}-\chi_{Pauli}-\chi_{core} . \quad (23)$$

Concerning χ_{Pauli}, we can use those obtained from the density of stages calculated from Ohno-Kamimura's band structure for first to sixth stage.[16] These values are in good agreement with those measured by Ikehata *et al.*[17] for first- to third-stage potassium GIC's using the ESR-NMR resonance method. As for χ_{core}, however, there are no direct experimental data. Therefore, in experimental analysis of Eq. (23) the calculated values of carbon and potassium atoms are used for χ_{core}. If the absolute value of χ_{core} in higher stage K GIC's is different from those estimated in experimental analysis, the experimental values of χ_{or} will change. In this respect, there is some ambiguity in the magnitude of experimental χ_{or}. Another reason for discrepancy lies in the thin film model. If the interlayer interactions between graphite layers across an intercalant layer is large, we must consider the effect of such interlayer interactions on χ_{or} which has not been taken into account in this paper.

IV. RESULTS FOR $f=0.3$ AND DISCUSSION

Now we turn to discussing the orbital susceptibility in the case of a small amount of charge transfer. For this purpose we have calculated the orbital susceptibility of stages 3 and 4 for the charge transfer of $f=0.3$. The results are shown in Fig. 6. In some of acceptor GIC's the absolute value of the charge transfer has been reported to be about 0.3.[18] Thus the present result of χ_{or} for $f=0.3$ may be compared with χ_{or} observed for some of acceptor compounds, because the band structure of acceptor GIC's with $f=-0.3$ is obtained from that with $f=0.3$ near the K point by changing the sign of energy simply. Ohno and Kamimura have shown that when the charge transfer is small, the c-axis charge distribution becomes less inhomogeneous, compared with that for $f=1.0$.[15] According to our formalism of the effective Hamiltonian, this tendency appears as the reduction in the value of δ, because the energy separation between various bands becomes smaller. In spite of reduction of the Fermi energy due to a smaller charge transfer, the Fermi energy for third stage with $f=0.3$ exists above the bottom of the highest conduction band. Furthermore, the band parameters of γ_1, γ_3, and γ_4 which were obtained by fitting the band structure of Ohno and Kamimura become smaller as listed in Table II. Consequently the orbital susceptibility of the third stage for $f=0.3$ is paramagnetic but its value is smaller by about 20% than that of $f=1.0$. A simple explanation of paramagnetism is due to the fact that the Fermi energy appears above the highest conduction bands and thus intraband interaction dominates. For the fourth stage the Fermi energy is located just below the conduction bands and thus the orbital susceptibility turns to be slightly diamagnetic. This situation is similar to that in the fifth stage with $f=1.0$.

So far the observations of orbital susceptibility of acceptor-type GIC's have been reported for second-stage $SbCl_5$ GIC's by Ikehata *et al.*[17] and for second- to fifth-stage $SbCl_5$ GIC's by Yoshida *et al.*[19] Ikehata *et al.* have shown that the paramagnetism of second-stage $SbCl_5$ GIC is much smaller than that of alkali GIC's while Yoshida *et al.* have shown that the second-stage $SbCl_5$ GIC is slightly diamagnetic and that χ_{or} decreases monotonously and also sharply as the stage number increases. The difference in the values of χ_{or} in the second stage between two experimental groups is due to the different estimation of core susceptibility of intercalants.[17,19] As far as the stage dependence of susceptibility is concerned, the agreement between experimental and calculated results is quite good. The agreement is better than that in the case of donor-type GIC's. A possible explanation for this may be as follows. In the acceptor GIC's the intercalants are usually large molecules and the separation of graphite layers across intercalant layers is sufficiently large. In that case the thin film model we adopted in this paper is a good approximation.

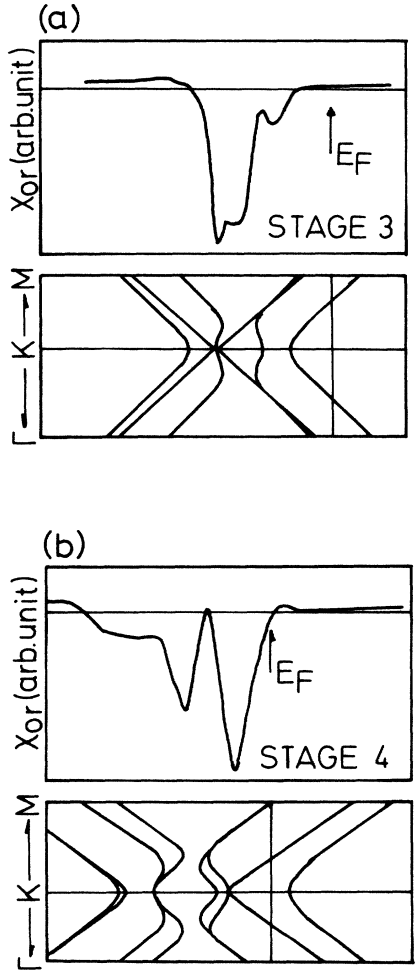

FIG. 6. Calculated results of the orbital susceptibility χ_{or} for $f=0.3$ as a function of the Fermi energy (upper part) and the expanded section of the energy dispersion near the K point for the third and fourth stage GIC's with $f=0.3$: (a) third stage and (b) fourth stage ($f=0.3$) (lower part).

V. CONCLUSIONS

In conclusion we have calculated the orbital susceptibility of the higher stage GIC's by taking into account the interlayer interactions. In doing so, we have developed a new formulation to calculate the orbital susceptibility of the multibands system such as the present GIC system. The computation of the orbital susceptibility was performed for donor-type GIC's from first- to fifth-stage GIC's with the charge transfer $f=1.0$ and for third- to fourth-stage GIC's with $f=0.3$, using the method of effective Hamiltonian. We have clarified the roles of both intraband and interband interactions in determining the orbital susceptibility. Especially we have shown that the band parameters γ_3 and γ_4 which cause the mixing of orbital angular momentum between different energy bands play important roles in enhancing the orbital paramagnetism. We have further shown that the orbital susceptibility has a maximum at the fourth stage in its stage dependence for $f=1.0$, and turns to be diamagnetic at the fifth stage. These results have explained the observed stage dependence satisfactorily. We have also shown that the orbital susceptibility takes a considerably smaller value when the charge transfer becomes smaller. In this connection we have suggested that in the case of acceptor GIC's with small charge transfer the orbital susceptibility becomes diamagnetic from lower stage.

ACKNOWLEDGMENTS

We would like to thank Dr. T. Ohno for helpful suggestions and discussions and also for his collaboration in the early stage of this work. We also express our gratitude to Professor H. Suematsu, Professor S. Ikehata, Dr. Y. Yoshida for variable discussions and for showing their experimental results prior to publication. We also thank Dr. S. A. Safran for sending a copy of his recent work on orbital susceptibility prior to publication. Part of this work was supported by the grants-in-aid of special research project on properties of molecular assemblies (No. 60104002) from the Ministry of Education, Science and Culture, Japan.

[1]F. J. DiSalvo, S. A. Safran, R. C. Haddon, J. V. Waszczak, and J. E. Fischer, Phys. Rev. B **20**, 4883 (1979); F. J. DiSalvo and J. E. Fischer, Solid State Commun. **28**, 71 (1978).

[2]J. W. McClure, Phys. Rev. **119**, 606 (1960).

[3]M. P. Sharma, L. G. Johnson, and J. W. McClure, Phys. Rev. B **9**, 2467 (1974).

[4]J. E. Fischer, C. D. Fuerst, and K. C. Woo, Synth. Met. **7**, 1 (1983).

[5]K. Suda and H. Suematsu (private communication).

[6]S. A. Safran and F. J. DiSalvo, Phys. Rev. B **20**, 4889 (1979).

[7]S. A. Safran, F. J. DiSalvo, R. C. Haddon, J. V. Waszczak, and J. E. Fischer, Physica B **99**, 494 (1980).

[8]H. Fukuyama, Prog. Theor. Phys. **45**, 704 (1971).

[9]J. Blinowski and C. Rigaux, J. Phys. (Paris) **45**, 545 (1984).

[10]S. A. Safran, Phys. Rev. B **30**, 421 (1984).

[11]A. A. Abrikosov, L. P. Gor'kov, and I. E. Dzyaloshinski, *Methods of Quantum Field Theory in Statistical Physics*, translated by R. A. Silverman (Prentice-Hall, Englewood Cliffs, 1963), Chap. 3.

[12]R. Saito, thesis, Tokyo University, 1985.

[13]J. Blinowski, Nguyen Hy Hau, C. Rigaux, J. P. Vieren, R. Le Toullec, G. Furdin, A. Herold, and J. Melin, J. Phys. **41**, 47 (1980).

[14]J. Blinowski and C. Rigaux, J. Phys. **41**, 667 (1980).

[15]T. Ohno and H. Kamimura, J. Phys. Soc. Jpn. **52**, 223 (1983).

[16]H. Kamimura, in *Extended Abstracts of GIC*, edited by P. C. Eklund, M. S. Dresselhaus, and G. Dresselhaus (Materials Research Society, Pittsburg, 1984), p. 36.

[17]S. Ikehata, H. Suematsu, and S. Tanuma, Solid State Commun. **50**, 375 (1984).

[18]L. Pietronero and S. Strassler, Phys. Rev. Lett. **47**, 593 (1981).

[19]Y. Yoshida, S. Tanuma, and Y. Iye, J. Phys. Soc. Jpn. **54**, 2635 (1985).

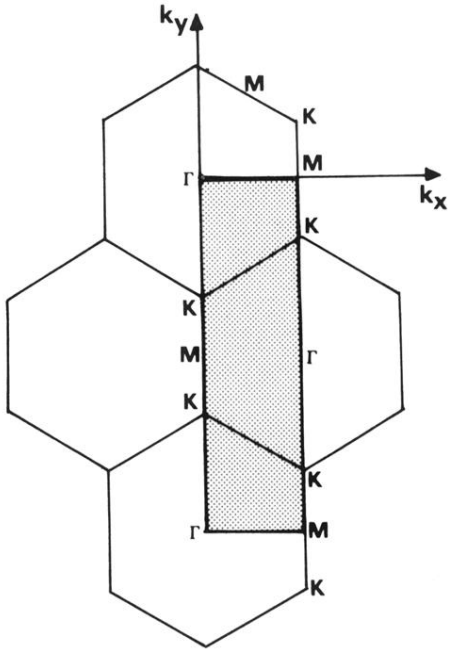

FIG. 2. Rectangle section in the extended zone of the reciprocal lattice adopted for the numerical integration. This section is equivalent to the hexagon of the first Brillouin zone.